

# An Experimental Investigation of Laser Transformation Hardening of Unalloyed Titanium Using Nd:YAG Laser

Dr. Duradundi. Sawant. Badkar

Department of Mechanical Engineering, Shri Balasaheb Mane Shikshan Prasarak Mandal Ambap's,  
Ashokrao Mane Group of Institutions, Vathar Tarf Vadgaon, Dist: Kolhapur -416112,  
Maharashtra State, India  
*email: dsbadkar@gmail.com*

**Abstract**—This research paper presents the investigation on laser transformation hardening (LTH) of unalloyed titanium of 1.6mm thickness sheet, nearer to ASTM Grade 3 of chemical composition was investigated using 2KW CW Nd:YAG Laser. The effects of laser process parameters: laser power(750-1250W), scanning speed (1000-3000 mm/min) and focal point position (-10mm to -30mm) on the hardened bead profile parameters such as hardened bead width (HBW) and hardened depth (HD) was investigated using Response Surface Methodology (RSM). The experimental design is based on an independent quadratic Box-Behnken Design (BBD) matrix. The reduced linear and quadratic polynomial equations for predicting hardened bead width and hardened depth of beadprofile were developed. Adequacies of models were examined by Analysis of Variance (ANOVA) technique. The results designate that the mathematical models developed predict the responses adequately adequate within the limits of hardening parameters being employed. It is recommended that the regression equations can be used to find optimum laser hardening conditions for desired criterion.

**Keywords**-Laser Transformation Hardening, Nd:YAG laser, Response Surface Methodology, Hardened Bead Profiler

\*\*\*\*\*

## I. INTRODUCTION

Titanium is a very attractive material for aerospace applications due to its low thermal conductivity, relatively low density and elastic modulus, light weight, high strength to weight ratio and temperature capabilities; titanium is used in cryogenic applications as well as for elevated temperature applications up to ~600°C. Titanium and its alloys are of excellent corrosion resistance, wear resistance, and high specific strength (strength/density), titanium and its alloys have been extensively used for chemical, electric power, marine, biomedical, pharmaceutical and aerospace industries as major metal materials by taking advantage of their characteristics. On the other hand, their applications to automobile industry have been limited except for racing cars and special-purpose cars because of their high cost despite the strong interest shown in titanium materials by the industry in terms of lightweight, fuel efficiency and performances. A unique aspect of titanium is that even the modulus can be modified by heat treatment and/or processing. The laser surface transformation hardening was initially reported in the early seventies and that has become an established technology in manufacturing and processing industries to improve the surface characteristics of intricate and selected areas of various engineering components. This has been revolutionizing automobile and aerospace industries for hardening surface layers of the turbine blades, crankshafts, piston ring grooves and tractor engine components, etc. Laser hardening process gives a wear-resistant surface layer, thereby increasing the service life of components to a considerable extent. All cast iron, medium-carbon steel and tool steel are amenable to the laser hardening process [1].

Laser Surface Transformation Hardening (LSTH) fundamentally allows obtaining a hardened surface layer in titanium and its alloys by changing the base structure into

hardened transformed beta martensite. Hardenability of titanium and its alloys is a phrase that refers to its ability to permit full transformation of the titanium and its alloys to transformed beta (martensites, alpha) or to retain beta to room temperature. The standard laser transformation hardening (LTH) of titanium and its alloys involves two main steps: 1. beta phase formation, in which the material is heated to/above the beta transus temperature, i.e.,  $\beta$ -transus (88 °C or 1621 °F), in order to form the material with 100% beta phase (but below the melting point) and 2. “self quenching” or cooling down, where  $\beta$ -phase is transformed into harder acicular (plate-like)  $\alpha$  martensite (transformed  $\beta$ ) or retain beta to room temperature. The  $\beta$ -transus is defined as the lowest equilibrium temperature at which the material is 100% beta or alpha, which does not exist. The  $\beta$ -transus is critical in deformation processing and in heat treatment. A correct treatment requires the heating stage long enough for the  $\beta$ -phase formation to complete and allow the alloying elements such as manganese, carbon, oxygen and nitrogen to stabilize it and dissolve iron, vanadium, molybdenum, copper, nickel and silicon into the matrix. Self quenching should be fast enough so as to suppress the normal breakdown of  $\beta$ -phase into the initial  $\alpha$  or ( $\alpha+\beta$ ) phases and produce hard plate like alpha martensite formation instead [2].

A high power laser beam can be delivered to the workpiece with a very precise spatially and temporally control. For the localized laser heating, bulk of the workpiece remains at a low temperature and acts as a heat sink and therefore, when laser irradiation is stopped, rapid self-quenching takes place. Compared to standard hardening procedures, the laser techniques offer several advantages. The applied laser radiation instantaneously heats a localized region on the surface and the bulk of the material acts as an efficient heat sink producing high cooling rates [3,4]. This

means that desired hardened depths can be achieved at high laser processing speeds and with minimal thermal distortion in the treated parts. In addition, it has been shown that laser surface hardening not only increase the wear and corrosion resistance but also increase the fatigue strength under certain conditions. [5, 6]. In this research, continuous wave 2kW, Nd:YAG laser source with radiation wavelength of 1.064  $\mu\text{m}$  has been used to produce hardening of commercially pure titanium nearly ASTM Grade 3 of 1.6mm thickness sheet.

From the literature survey it has been observed that many authors have published their research work related to only laser welding, cladding, cutting, hardening processes specifically steel materials with full factorial design, Box-Behnken design, Plackett-Burman design, and Central Composite Design using RSM. Prachya Peasura studied the application of the Response Surface Methodology (RSM) and Central Composite Design (CCD) experiment in mathematical model and optimizes post weld heat treatment (PWHT). Author found the influence of PWHT and the most appropriate mathematical model as the basis for further ASTM A516 grade 70 weld applications using response surface methodology (RSM) to find the optimal parameters and the central composite design (CCD) experimental design for a mathematical model to predict the tensile strength [7]. D. S. Badkar, et al. investigated the influence of laser phase transformation hardening parameters on heat input and hardened-bead profile quality of unalloyed titanium using Nd: YAG laser. The applied the response surface methodology (RSM) in order to develop the mathematical modeling of heat input and angle of entry of hardened bead geometry [1]. Duradundi Sawant Badkar et al. investigated and evaluated the optimal values of laser process parameters: laser power, scanning speed, and focused position for the simultaneous minimization and maximization of heat input and tensile strength respectively by Taguchi method and utility concept approach in laser transformation hardening of commercially pure titanium sheet of 1.6mm thickness using continuous wave (CW) Nd:YAG laser beam [8]. Duradundi Sawant Badkar employed a Full Factorial Design (FFD) with Response Surface Methodology (RSM) to establish, optimize and to investigate the relationships of three laser transformation hardening process parameters: laser power, scanning speed, and focused position on laser hardened bead profile parameters such as angle of entry of hardened bead profile and power density. RSM is used to develop pseudo-closed-form models from the computational parametric studies. The results demonstrate that the developed models are accurate with low percentages of error [9]. Duradundi Sawant Badkar studied the effect of laser process variables such as laser power, scanning speed, and focused position was investigated using response surface methodology (RSM) and artificial neural network (ANN) keeping argon gas flow rate of 10 lpm as fixed input parameter. This paper describes the comparison of the heat input (HI) and ultimate tensile strength ( $\sigma$ ) (simply called as tensile strength) predictive models based on ANN and RSM. The paper also presents the effect of laser process variables on the HI and ultimate  $\sigma$ . The research work also emphasizes on the effect of HI on  $\sigma$ . The experiments were conducted based on a three-factor, three-level Box-Behnken surface statistical design. Quadratic polynomial equations were developed for proper

process parametric study for its optimal performance characteristics [10].

Duradundi Sawant Badkar et al. in their study applied the Response Surface Methodology (RSM) and Central Composite Design (CCD) for modeling, optimization, and an analysis of the influences of dominant laser-processing parameters namely: laser power (LP), scanning speed (SS), and focused position (FP) on heat input (HI) and hardened bead geometries such as hardened bead width (HBW), hardened depth (HD), angle of entry of hardened bead profile (AEHB) of laser transformation hardened surface quality of commercially pure titanium sheet of 1.6 mm in thickness using continuous wave (CW) 2-kW Nd:YAG laser. They showed the predicted results are compared with the experimental results and are good agreement with heat input and hardened bead profile parameters [11]. Duradundi Sawant Badkar et al. developed the mathematical models from Response Surface Methodology (RSM) are used to predict the laser phase transformation hardened bead profile parameters in terms of the laser process factors; namely laser power (LP), scanning speed (SS) and focused position (FP), used to optimize the laser transformation hardening process. It has been investigated that the results accomplished from both numerical optimization and graphical methods ensured almost analogous values to each other for optimal LTH conditions in all the cases [12].

In this research article author has made an effort in establishing the influence of laser process parameters on hardened bead geometry, and developing the mathematical models in order to optimize the laser process parameters thereby achieving the hardened bead geometry with maximum hardened bead width and minimum hardened depth.

## II. EXPERIMENTAL DESIGN

The experimental design is based on a three level Box-Behnken design with full replication [13]. Box-Behnken designs are response surface designs specially made to require only 3 levels, codes as -1, 0, and +1. Table 1 shows laser input variables and experimental design levels used.

A response surface method (RSM) has been often applied to optimize the formulation variables [14, 15]. RSM designs allow us to estimate interaction and even quadratic effects, and hence give us an idea of the (local) shape of the response surface under investigation. The optimization procedure based on RSM includes statistical experimental designs, multiple regression analysis, and mathematical optimization algorithms for seeking the best formulation under a set of constrained equations. RSM was applied to the experimental data using statistical software, Design-expert 7. Linear and second order polynomials were fitted to the experimental data to obtain the regression equations. The sequential F-test, lack-of-fit test and other adequacy measures were used in selecting the best models. A step-wise regression method was used to fit the second order polynomial equation (1) to the experimental data and to identify the relevant model terms [16, 17]. The same statistical software was used to generate the statistical and response plots. The second-order model is utilized to find a suitable approximation for the functional relationship between independent variables and the response surface.

$$Y = \beta_0 + \sum_{i=1}^k \beta_i X_i + \sum_{i=1}^k \beta_{ii} X_{ii} + \sum_{i=1}^k \sum_{j=i+1}^k \beta_{ij} X_i X_j + \varepsilon \quad (1)$$

where  $Y$  is the response calculated by model (dependent variables),  $\beta_0$  is the constant coefficient,  $\beta_i$  are the coefficients for the linear effect,  $\beta_{ij}$  are the coefficients for the quadratic effect,  $\beta_{ijk}$  are the coefficients for the cross-product effect,  $X_{ij}$ ,  $X_j$  are the variables corresponding to factors (independent variables),  $\epsilon$  is the error,  $k$  the number of variables considered and  $i, j$  are the factors.

III. EXPERIMENTAL METHODOLOGY

The experiments are conducted on a given unalloyed Titanium alloy substrate with chemical composition given in Table 2. The chemistry is nearer to ASTM Gr. 3. The thickness of the substrate selected is 1.6 mm, to simulate the majority of the industrial applications that is in practice at present. For conducting the experiments on the substrate, the materials surface is cleaned properly with suitable agents.

TABLE 1. PROCESS TITANIUM VARIABLES AND EXPERIMENTAL DESIGN LEVELS USED

Variables	-1	0	+1
Laser power, LP(Watts)	750	1000	1250
Scanning speed, SS (mm/min)	1000	2000	3000
Focused position, FP (mm)	-30	-20	-10

TABLE 2. CHEMICAL COMPOSITION OF UNALLOYED

Ele.	Ti	C	Fe	Mo	V	Cu	O	Al
% By Wt	Bal.	0.011	0.15	0.003	0.029	0.14	0.1	1.1



Figure 1. Solid state Nd:YAG Laser source at WRI used for experimental work [18].

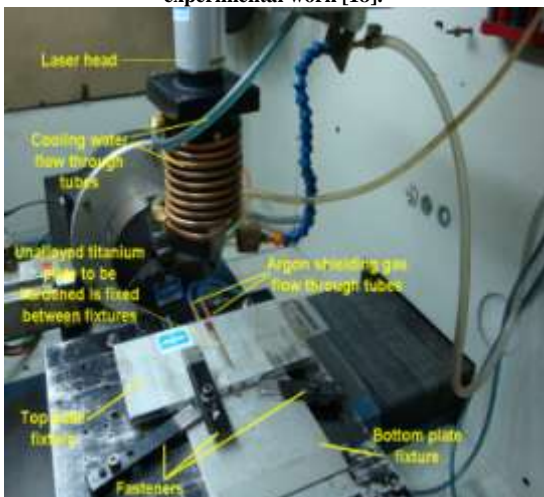


Figure 2. Experimental set-up showing the laser beam head and shielding arrangements in the working chamber [18].

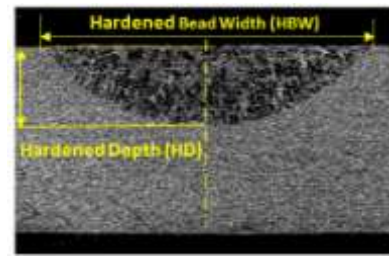


Figure 3. Microstructure of Hardened - Bead Profile with parameters,

Exp No	Run order	Coded variables			Actual variables		
		LP (Watts)	SS (mm/min)	FP (mm)	LP (Watts)	SS (mm/min)	FP (mm)
1	14	-1	-1	0	750	1000	-20
2	1	1	-1	0	1250	1000	-20
3	4	-1	1	0	750	3000	-20
4	8	1	1	0	1250	3000	-20
5	3	-1	0	-1	750	2000	-30
6	5	1	0	-1	1250	2000	-30
7	6	-1	0	1	750	2000	-10
8	16	1	0	1	1250	2000	-10
9	10	0	-1	-1	1000	1000	-30
10	13	0	1	-1	1000	3000	-30
11	7	0	-1	1	1000	1000	-10
12	15	0	1	1	1000	3000	-10
13	12	0	0	0	1000	2000	-20
14	11	0	0	0	1000	2000	-20
15	9	0	0	0	1000	2000	-20
16	17	0	0	0	1000	2000	-20
17	2	0	0	0	1000	2000	-20

HBW, HD and AEHB

TABLE 3. DESIGN MATRIX WITH CODE INDEPENDENT PROCESS VARIABLES

A continuous wave (CW) 2KW, with radiation wavelength  $\lambda=1.06\mu\text{m}$  Nd: YAG laser source from GSI Lumonics is employed for the experimental work as shown in Fig.1. The experiment was carried out according to the design matrix in a random order to avoid any systematic error. A spherical beam configuration is used throughout for the study. The experiment set up is shown in Fig.2. The laser beam is transported through a fibre optic cable to the work centre. Siemens 802 CNC controller is providing the process control during the experiments. The work centre is having x, y and rotational movement for processing applications. The laser source, work centre and the controls are interfaced. Cooling is ensured by a chiller and a cooling tower. For the study, 120mm focal optic is employed with varying beam spot size depending on defocus distance to obtain a wider scan area. Argon gas is employed as shielding medium with a constant flow rate of 8lpm throughout the experimental work. Transverse sectioned specimens were cut from laser hardened bead-on trial of unalloyed titanium sheet and mounted. Standard metallographic was made for each transverse sectioned specimens. The bead profile parameters ‘responses’ were measured using an optical microscope (with Image processing computer controlled software) with digital micrometers attached to it with an accuracy of 0.001 mm, which allow to measure in x-axes and y-axes directional movement.

Fig.3 shows microstructure of laser Hardened-Bead Profile with measured parameters, such as hardened bead width (HBW), hardened depth (HD) and angle of entry of hardened bead profile(AEHB) for CW spherical beam. The



measured laser hardened bead profile parameters ‘responses’ were recorded. The design matrix is shown in Tables 3.

IV. RESULTS AND DISCUSSION

The results of the laser hardened-bead on trials were measured according to the design matrix with coded and actual independent process variables in Table 3 using the transverse sectioned specimens and the optical microscope mentioned earlier, the measured responses are listed in Table 4. Analyzing the measured responses by the Design-expert software, the fit summary output indicates that the linear model is significantly significant for hardened bead width (HBW) ‘the second response’ therefore it will be used for further analysis. While for the other response hardened depth (HD) the quadratic models is statistically and is recommended for the further analysis.

A. Analysis of variance (ANOVA)

The adequacy of the developed models were tested using the analysis of variance (ANOVA) technique and the results of the linear and quadratic order response surface model fitting in the form of analysis of variance(ANOVA) are given in Tables 4-5. The test for significance of the regression models, the test for significance on individual model coefficients and the lack-of-fit test were performed using the same statistical Design-expert 7 software package. By selecting the step-wise regression method, which eliminates the insignificant model terms automatically, the resulting ANOVA Tables 4-5 for the response surface quadratic models summarize the analysis of variance of each response and show the significant model terms.

The same Tables show also the other adequacy measures  $R^2$ , adjusted  $R^2$  and predicted  $R^2$ . The coefficient of determination  $R^2$  indicates the goodness of fit for the model. In this case, all the values of coefficient of determination  $R^2$  are nearly equal to 1. Clearly, we must have  $0 \leq R^2 \leq 1$ , with larger values being more desirable. The adjusted coefficient of determination  $R^2$  or “adjusted”  $R^2$  is a variation of the ordinary  $R^2$  statistic that reflects the number of factors in the model. The entire adequacy measures are closer to 1, which is in reasonable agreement and indicate adequate models. The adequate precision “Adeq Precision” compares the range of the predicted value at the design points to the average prediction error. Adequate precision measures signal to noise ratio. A ratio greater than 4 is desirable. In all cases the value of adequate precision are dramatically greater than 4. The adequate precision ratio above 4 indicates adequate model discrimination. The ANOVA Tables 5-6 also shows the model terms standard Std. Dev, Mean, C.V and PRESS. “Std. Dev.” Standard deviation is a square root of the error mean square,  $(\sqrt{MS_E})$  and “C.V.” is the coefficient of variation, defined  $(\sqrt{MS_E} / \bar{y})$  100, where  $\bar{y}$  = Mean. The coefficient of variation, “C.V” measures the unexplained or residual variability in the data as a percentage of the mean of the response variable. At the same time a relatively lower values of the coefficient of variation, C.V., from the Tables 4-5 indicate improved precision and reliability of the conducted experiments. “PRESS” stands for “Prediction Error Sum of Squares,” and it is a measure of how well the model for the experiment is likely to predict the responses in a new experiment. Small values of PRESS

are desirable. In all the cases the values of PRESS are considerably small. The values of “Probability > F” in Tables 4-5 for all models are less than 0.0500 indicate that all models are significant. In all cases the “Lack-of-fit” values implies the “Lack-of-fit” is not significant relative to the pure error. Non-significant lack- of- fit as it is desired and it is good.

The analysis of variance for the hardened bead width (HBW) model, from the Table 4 the analysis indicated that there is a linear relationship between the main effects of the three process parameters. Also, in the case of hardened depth (HD) model, from the Table 5 the main effect of laser power (LP), scanning speed (SS), focused position (FP), interaction effect of laser power (LP) with scanning speed (SS) and the second order effect of scanning speed (SS) have the significant effect.

TABLE 4. ANOVA TABLE FOR THE HARDENED BEAD WIDTH REDUCED LINEAR MODEL

Source	Sum of Squares	df	Mean Square	F Value	p-value Prob > F	
Model	1.2231	3	0.4077	157.3093	< 0.0001	Sig.
LP	0.6699	1	0.6699	258.4824	< 0.0001	
SS	0.5045	1	0.5045	194.6655	< 0.0001	
FP	0.0487	1	0.0487	18.78011	0.0008	
Residual	0.0337	13	0.0026			
Lack of Fit	0.0227	9	0.0025	0.922208	0.5804	not sig.
Pure Error	0.011	4	0.0027			
Corrected Total	1.2568	16				

Std. Dev.	0.0509	R-Squared	0.9732
Mean	2.2522	Adj R-Squared	0.9670
C.V. %	2.2604	Pred R-Squared	0.9533
PRESS	0.0587	Adeq Precision	43.775

TABLE 5. ANOVA TABLE FOR HARDENED DEPTH REDUCED QUADRATIC MODEL

Source	Sum of Squares	df	Mean Square	F Value	p-value Prob > F	
Model	0.9284	5	0.1857	61.4275	< 0.0001	Sig.
LP	0.2309	1	0.2309	76.3746	< 0.0001	
SS	0.6166	1	0.6166	203.989	< 0.0001	
FP	0.0164	1	0.0164	5.4191	0.0400	
LP×SS	0.0195	1	0.0195	6.43796	0.0276	
SS2	0.0451	1	0.0451	14.9169	0.0026	
Residual	0.0333	11	0.003			
Lack of Fit	0.0153	7	0.0022	0.48566	0.8099	not sig.
Pure Error	0.018	4	0.0045			
Corrected Total	0.9616	16				

Std. Dev.	0.0549	R-Squared	0.9654
Mean	0.6370	Adj R-Squared	0.9497
C.V. %	8.63099	Pred R-Squared	0.9069
PRESS	0.0895	Adeq Precision	27.4010

TABLE 6. CONFIRMATION OF EXPERIMENTS

Exp No	Process parameters	Responses	Actual value	Predicted value	Error	Error %
1	LP=750Watts SS=3000mm/min FP=-30mm	HBW (mm)	1.792	1.78974	0.002	0.112
		HD (mm)	0.259	0.26863	-0.010	-3.861
2	LP=1250Watts SS=2000mm/min FP=-20mm	HBW (mm)	2.425	2.542	-0.117	-4.820
		HD (mm)	0.724	0.758	-0.034	-4.690

3	LP=1250Watts SS=3000mm/min FP=-30mm	HBW (mm)	2.274	2.368	-0.094	-4.130
		HD (mm)	0.440	0.469	-0.029	-6.590
4	LP=1000Watts SS=1000mm/min FP=-20mm	HBW (mm)	2.519	2.503	0.001	0.630
		HD (mm)	1.043	0.969	0.074	7.090
5	LP=750Watts SS=1000mm/min FP=-30mm	HBW (mm)	2.274	2.292	-0.018	-0.791
		HD (mm)	0.716	0.684	0.032	4.470

The final mathematical models in terms of coded factors/variables as determined by design expert software are shown below:

$$\text{Hardened bead width (HBW)} = 2.2522 + 0.2894 \times \text{LP} - 0.251 \times \text{SS} - 0.078 \times \text{FP} \quad (2)$$

$$\text{Hardened depth (HD)} = 0.5884 + 0.1698 \times \text{LP} - 0.2776 \times \text{SS} + 0.0452 \times \text{FP} - 0.0697 \times \text{LP} \times \text{SS} + 0.1032 \times \text{SS}^2 \quad (3)$$

While the following final empirical models in terms of actual factors/variables:

$$\text{Hardened bead width (HBW)} = 1.441 + 0.00116 \times \text{LP} - 0.0002511 \times \text{SS} - 0.0078 \times \text{FP} \quad (4)$$

$$\text{Hardened depth (HD)} = 0.40941 + 0.00123 \times \text{LP} - 0.00041 \times \text{SS} + 0.00452 \times \text{FP} - 2.79 \times 10^{-7} \times \text{LP} \times \text{SS} + 1.032 \times 10^{-7} \times \text{SS}^2 \quad (5)$$

The above obtained mathematical models in terms of coded factors/variables (equation. 2 & equation. 3) are related to the coded laser process parameters and empirical models in terms of actual factors/variables (equation. 4 & equation.5) are related to the actual (experimental) values of laser process parameters. By substituting the related values of coded variables and corresponding equivalent values of actual (experimental) variables of laser processing parameters in the mathematical models in terms of coded factors and empirical models in terms of actual factors the corresponding output values of HBW and HD will be almost similar for the developed models of coded and actual factors/variables.

### B. Validation of the Models

Figs.4-5 show the relationship between the actual and predicted values of hardened bead width (HBW) and hardened depth (HD) of hardened bead profile respectively. These Figures indicate that the developed models are adequate because the residuals in prediction of each response are minimum, since the residuals tend to be close to the diagonal line. Furthermore, to verify the adequacy of the developed models, five confirmation experiments were carried out using new test conditions, but are within the experimental range defined early. Using the point prediction option in the software, the HI and HBW of the validation experiments were predicted using the previous developed models. Table 6 summarizes the experiments condition, the actual experimental values, the predicted values, error and the percentages of error.

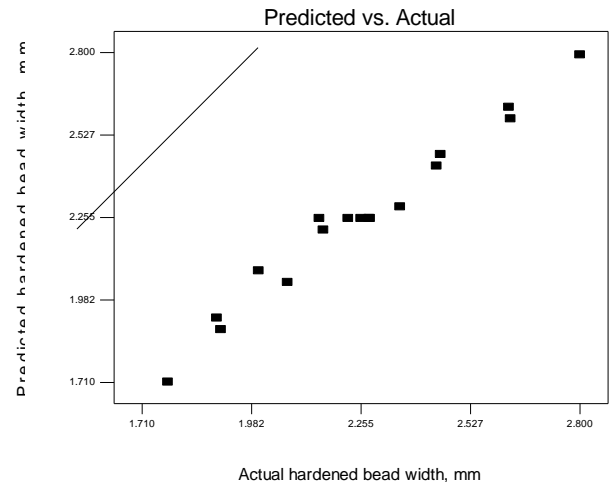


Figure 4. Scatter diagram of hardened bead width (HBW)

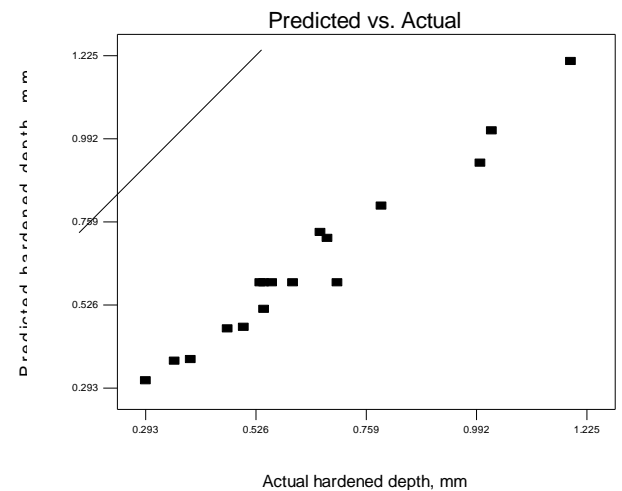


Figure 5. Scatter diagram of hardened depth (HD)

### C. Effect of Process Factors on Hardened-Bead Parameters

#### C.1. Hardened bead width (HBW)

Figs 6-11 show the effect of process parameters on the hardened bead width (HBW). From the results it is clear that the two parameters laser power (LP) and scanning speed (SS) are significantly affecting the hardened bead width (HBW) as compared to focused position (FP). From the Figs. 6 and 7, it is evident that the hardened bead width linearly increases with increasing LP and decreasing SS. At lower beam travel speed the time available for the laser beam to direct contact with the surface is more and hence hardened bead width increases. Therefore the heat input decreases leading to the less volume of the base being melted, consequently the width of the hardened zone decreases. From the Figs. 8 and 9 it is clear that as LP increases and FP decreases the hardened bead width (HBW) increases. Moreover, increase in defocused beam, or decrease in focused position i.e. from -10 mm, -20 mm, and -30 mm respectively means wide laser beam results in spreading the laser power onto wide area. Therefore, wide area of the base metal will melt leading to an increase in HBW or vice-versa. From the Figs. 10 and 11 it is observed that as the SS decreases and the FP decreases (i.e. from -10 mm to -30 mm) the hardened bead width increases.

The results show also that laser power (LP) plays very important role in the hardened bead dimensions. An increase in LP results in increase the HBW, because of increase in the power density.

C.2. Hardened depth (HD)

From the results it is studied that the parameters those significantly affecting the hardened depth are LP and SS. Effect of focused position on hardened depth is significant bur it has less influence as compared to LP and SS. These effects are due to following reasons: the increase in LP leads to an increase in the heat input, therefore, more molten metal and consequently more HD will be achieved. However, the idea is reversed in case of SS effect, because the SS matches an opposite with heat input (HI). From the Figs 12 and 13 it is seen that HD increases as LP increases and SS decreases. It is very important to note that in case of laser transformation hardening process main aim is to harden the surface with desired optimum depth. As much as possible instead of focusing the beam it is convenient to have defocused beam with negative focal length (i.e. from -10 mm, -20 mm and -30 mm), hence there is no loss of heat energy of laser beam above the focal point, since the laser beam is of converging type. Therefore laser heat input with minimum loss will be converged and concentrated on a specified localized area with desired hardened bead width and depth without spreading of laser power is achieved. Below the focal point or focused beam, the laser beam is of divergent type, results in spreading of laser power with maximum loss of heat input energy. Using a focused beam results in increasing the power density, which mean the heat will localize in small portion results in increasing in power density leading to better hardened bead width and depth which is desirable for laser transformation hardening (LTH). Therefore, due to the above reasons mentioned, it may be noted that to achieve the desired optimum hardened width and depth it is most convenient to have defocused laser beam with negative focal length ( i.e. above the focal point) for example -10 mm, -20 mm and -30 mm.

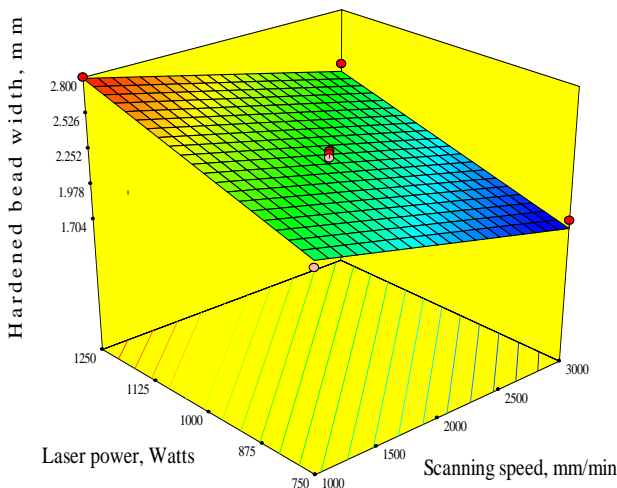


Figure 6. 3Dgraph shows the effect of LP and SS on the hardened bead width

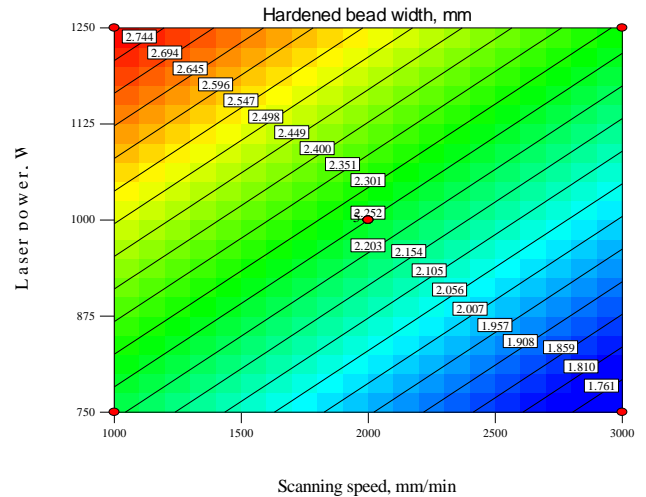


Figure 7. Contours graph shows the effect of LP and SS on the hardened bead width

From the Figs.12 and 13 it is clear that hardened depth (HD) increases with increase in LP and decrease in SS. From the Figs.14 and 15, as LP decreases and defocusing increases (i.e FP from -10 to -30 mm) the HD decreases. It is also observed from the Figs.16 and 17, it is evident that as SS increases, hardened depth (HD) decreases considerably and as FP increases hardened depth (HD) decreases marginally. From the results obtained in Table 4 and from Figs.12-17, it is important to note that there is no large variation in the data of hardened depth (HD). Referring the Table 4 the range of HD lies between 0.293-1.191 mm and is of 0.898 mm variation only.

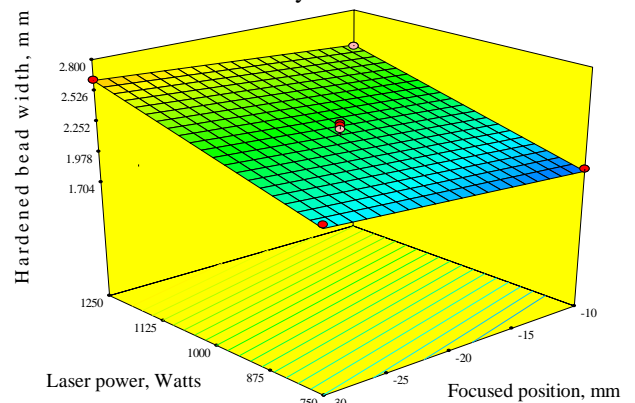


Figure 8. 3Dgraph shows the effect of LP and FP on the hardened bead width

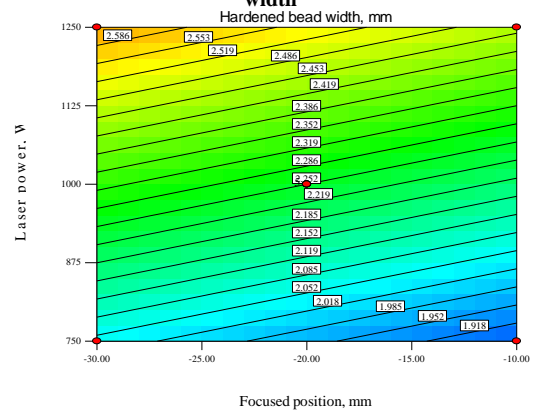


Figure 9. Contours graph shows the effect of LP and FP on the hardened bead width

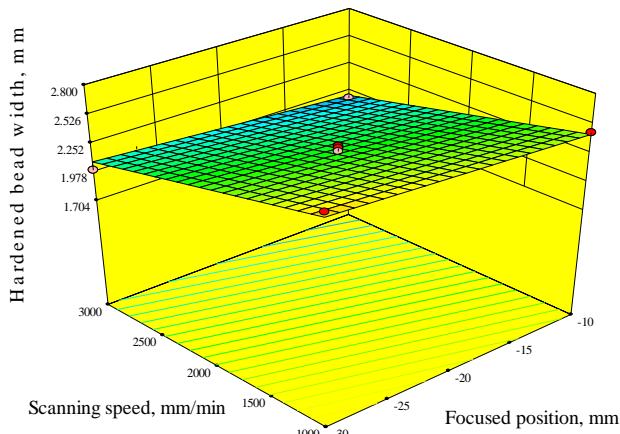


Figure 10. 3Dgraph shows the effect of SS and FP on the hardened bead width

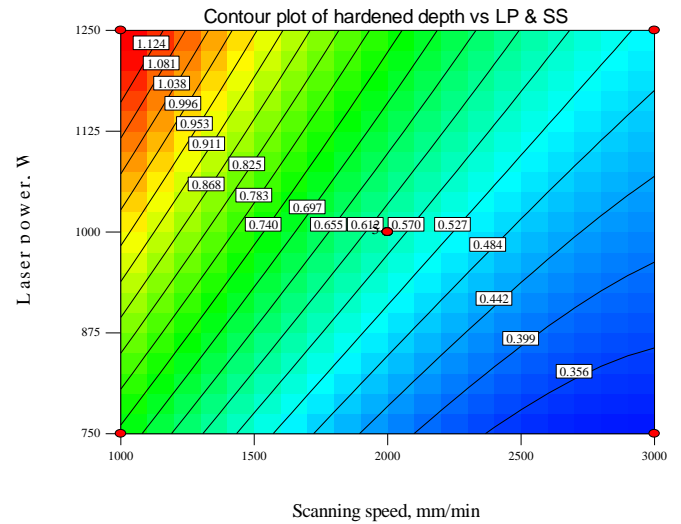


Figure 13. Contours graph shows the effect of LP and SS on the hardened depth

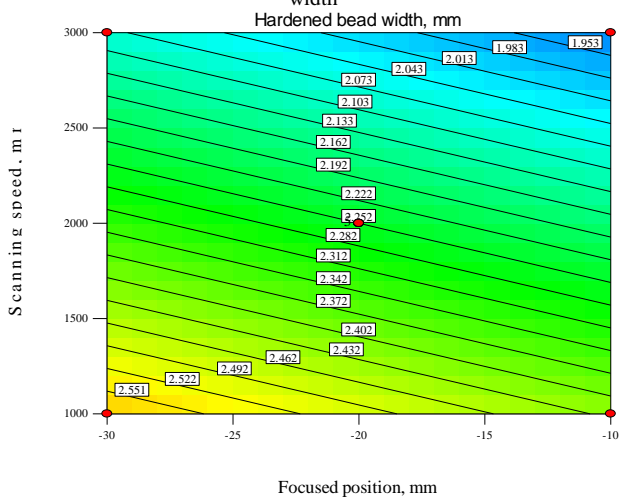


Figure 11. Contours graph shows the effect of SS and FP on the hardened bead width

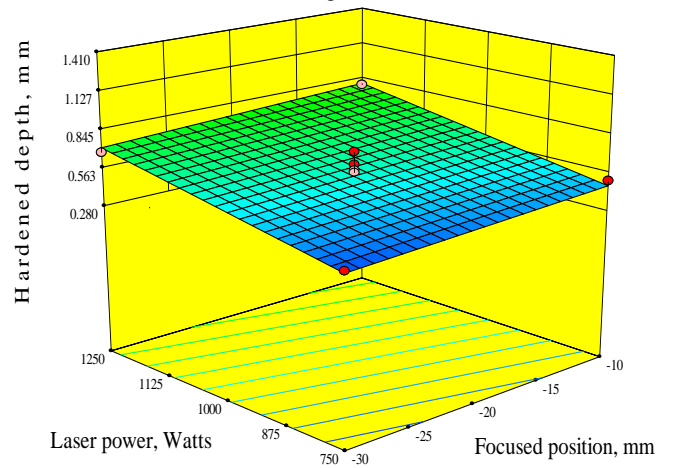


Figure 14. 3Dgraph shows the effect of LP and FP on the hardened depth

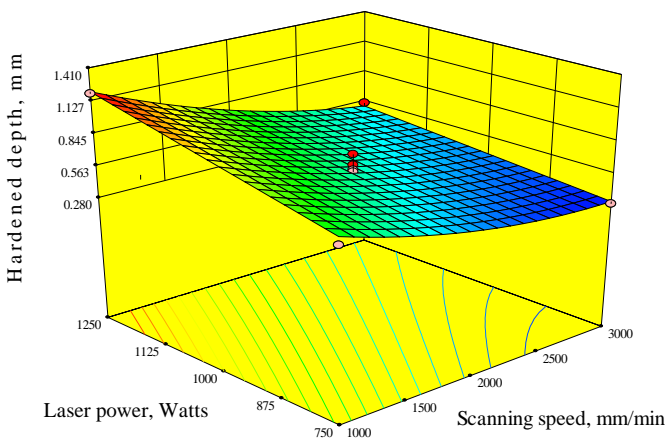


Figure 12. 3Dgraph shows the effect of LP and SS on the hardened depth

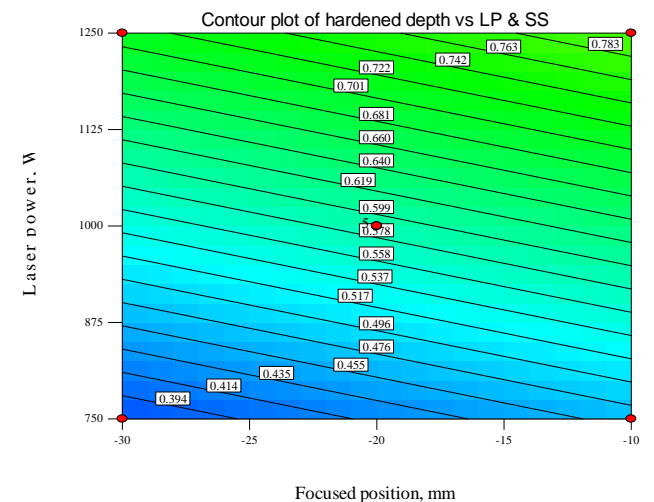


Figure 15. Contours graph shows the effect of LP and FP on the hardened depth



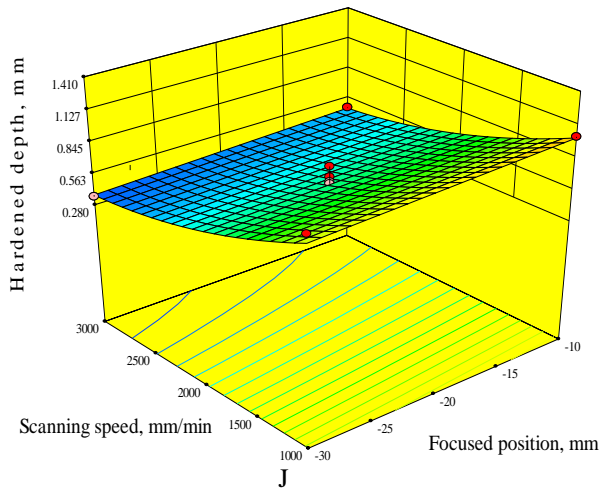


Figure 16. 3Dgraph shows the effect of SS and FP on the hardened depth  
Contour plot of hardened depth vs LP & SS

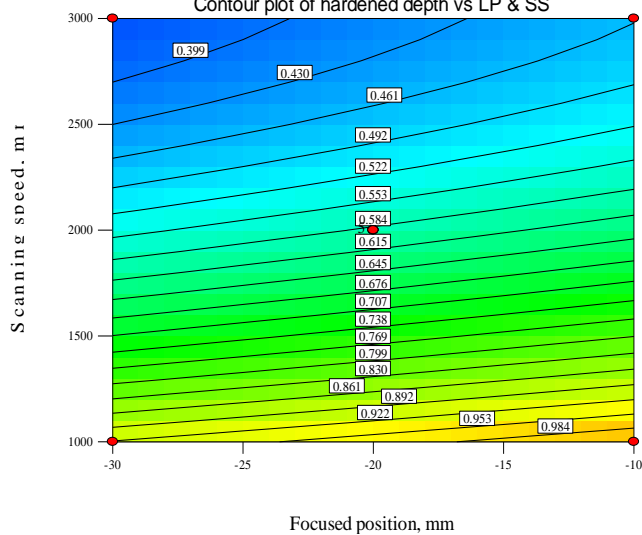


Figure 17. Contours graph shows the effect of SS and FP on the hardened depth

## V. CONCLUSIONS

The following conclusions were drawn from this investigation within the factors limits considered. This paper has described the use of Design of Experiments (DoE) for conducting the experiments. Four models were developed for predicting the heat input (HI), hardened bead width (HBW), hardened depth(HD), and angle of entry of hardened bead profile (AEHB) of the laser transformation hardened unalloyed titanium using response surface methodology(RSM). The following conclusions were drawn from this investigation within the factors limits considered.

1. Box-Behnken design can be employed to develop mathematical models for predicting laser hardened- bead geometry.
2. The desired hardened depth and width with high quality of laser transformation hardening (LTH) can be achieved by choosing the working condition using the developed models.
3. It is investigated that, in case of laser transformation hardening (LTH) though, as scanning speed increases depth of hardening decreases and vice-versa, but we are concentrating on desired optimum minimum depth.

Therefore, both scanning speed and laser power have positive effect on all the responses investigated.

4. Bead width as well as depth of hardening linearly decreases with increasing scanning speed.
5. It is evident that the bead geometry provides a useful tool to manipulate the hardened bead width and hardened depth during LTH. It is clearly observed that the hardened width linearly increases defocused beam i.e. with higher beam spot size. Depth of hardened surface increases linearly with decrease in defocused position from -30 mm to -10 mm.

## ACKNOWLEDGEMENTS

The authors thank the management of welding Research Institute, BHEL, Tiruchirappalli- 620 014, Tamil Nadu, India for allowing to work in the area of laser materials processing and the constant encouragement received from the faculties of MANIT Bhopal during the course of work.

## REFERENCESS

- [1]. Duradundi Sawant Badkar,Krishna Shankar Pandey,G. Buvanashekar an, “Effects of laser phase transformation hardening parameters on heat input and hardened-bead profile quality of unalloyed titanium”, Transactions of Nonferrous Metal Society China, Vol. 20, 2010, pp.1078–1091.
- [2]. Duradundi Sawant Badkar,Krishna Shankar Pandey,G. Buvanashekar an, “Laser Transformation Hardening of Unalloyed Titanium Using Nd: YAG laser”, International Journal of Material Science, Vol. 4(3), 2009, pp.239–250.
- [3]. J.M. Robinson, B.A. Van Brussel, J. Th. M. Dettosson and R.C.Reed, “X-ray measurement of residual stresses in laser surface melted Ti-6Al-4V alloy”, Material Science Engg, Vol.A208, 1996, pp.143-147.
- [4]. S.Zhang, W.T.Wu, M.C.Wang and H.C. Man, “In-situ synthesis and wear performance of TiC particle reinforced composite coating on alloy Ti6Al4V”, Surface Coating Technologies, Vol.138, 2001, pp.95-100.
- [5]. K.H.Lo, F.T.Cheng, H.C.Man, “Laser transformation hardening of AISI 440C martensitic stainless steel for higher cavitation erosion resistance, Surface Coating Technology”, Vol.173(1), 2003, pp. 96-104.
- [6]. D.I.Pantelis, E.Bouylouri, N. Kouloumbi, P.Vassiliu, A.Koutsomichalis, “Wear and corrosion resistance of laser surface hardened structural steel”, Surface Coating Technology, Vol.161 (2-3), 2002, pp.125-134.
- [7]. Prachya Peasura “Application of Response Surface Methodology for Modeling of Postweld Heat Treatment Process in a Pressure Vessel Steel ASTM A516 Grade 70”, The Scientific World Journal, Vol.2015, 2015, pp.1-8.
- [8]. Duradundi Sawant Badkar,Krishna Shankar Pandey, G. Buvanashakaran, “Multiperformance optimization of tensile strength and heat input of laser transformation hardening of commercially pure titanium using taguchi methodology and utility concept”, Advances in Production Engineering & Management, Vol.7 (3), 2012, pp. 165-176.
- [9]. Duradundi Sawant Badkar “Study on laser hardening parameters of ASTM Grade 3 pure titanium on an angle of entry of hardened bead profile and power density”, International Research Journal of Materials Science and Engineering, Vol. 3(1), 2017, pp. 19-34.
- [10]. Duradundi Sawant Badkar, Krishna Shankar Pandey, G. Buvanashakaran, “Development of RSM- and ANN-based models to predict and analyze the effects of process parameters of laser-hardened commercially pure titanium on heat input and tensile strength”, International Journal of Advanced Manufacturing Technology, Vol. 65 (9-12), 2013, pp.1319-1338.



- 
- [11]. Duradundi Sawant Badkar, Krishna Shankar Pandey, G. Buvanashakaran, "Application of the central composite design in optimization of laser transformation hardening parameters of commercially pure titanium using Nd:YAG laser", The International Journal of Advanced Manufacturing Technology, Vol. 59(1-4), 2012, pp.169-192.
- [12]. Duradundi Sawant Badkar, Krishna Shankar Pandey, G. Buvanashakaran, "Prediction and Optimization of Laser Transformation Hardening Parameters of Unalloyed Titanium Using RSM", Journal of Materials and Metallurgical Engineering, Vol. 5(1), 2015, pp.1-11.
- [13]. Design- expert software, version 7.1.6, User's Guide, Technical Manual, Stat-Ease Inc., 2009, Minneapolis, MN.
- [14]. Levison KK, Takayama K, Isowa K, Okaba K, Nagai T, Formulation optimization of indomethacin gels containing a combination of three kinds of cyclic monoterpenes as percutaneous penetration enhancers. J Pharm Sci.; 83(9) 1994, pp.1367-1372.
- [15]. Shirakura O, Yamada M, Hashimoto M, Ishimaru S, Takayama K, Nagai T, 1991, Particle size design using computer optimization technique. Drug Dev Ind Pharm.; 17(4), 1991, pp.471-483.
- [16]. Douglas. C. Montgomery, Design and data Analysis of Experiments, 5<sup>th</sup> ed., 2001, John Wiley & sons, New York Inc.
- [17]. A.I. Khuri, J.A. Cornell, Response Surfaces Design and Analysis, 2<sup>nd</sup> ed., 1996, Marcel Dekker, New York.
- [18]. Laser Materials Processing Lab, 2008, Welding Research Institute, BHEL, Tiruchirappalli-620015, Tamil Nadu, India.